tvst

https://doi.org/10.1167/tvst.7.2.14

Article

Evaluation of a Region-of-Interest Approach for Detecting Progressive Glaucomatous Macular Damage on Optical Coherence Tomography

Zhichao Wu[1–3], Denis S. D. Weng[1], Abinaya Thenappan[1], Robert Ritch[4], and Donald C. Hood[1,5]

[1] Department of Psychology, Columbia University, New York, NY, USA
[2] Centre for Eye Research Australia, Royal Victorian Eye and Ear Hospital, East Melbourne, Australia
[3] Ophthalmology, Department of Surgery, The University of Melbourne, Melbourne, Australia
[4] Einhorn Clinical Research Center, New York Eye and Ear Infirmary of Mount Sinai, New York, NY, USA
[5] Department of Ophthalmology, Columbia University, New York, NY, USA

Correspondence: Zhichao Wu, Centre for Eye Research Australia, Level 7, 32 Gisborne St, East Melbourne, VIC 3002, Australia. e-mail: wu.z@unimelb.edu.au

Received: 27 November 2017
Accepted: 11 February 2018
Published: 29 March 2018

Keywords: glaucoma; optical coherence tomography; progression; macula

Citation: Wu Z, Weng DSD, Thenappan A, Ritch R, Hood DC. Evaluation of a region-of-interest approach for detecting progressive glaucomatous macular damage on optical coherence tomography. Trans Vis Sci Tech. 2018;7(2):14, https://doi.org/10.1167/tvst.7.2.14

Purpose: To evaluate a manual region-of-interest (ROI) approach for detecting progressive macular ganglion cell complex (GCC) changes on optical coherence tomography (OCT) imaging.

Methods: One hundred forty-six eyes with a clinical diagnosis of glaucoma or suspected glaucoma with macular OCT scans obtained at least 1 year apart were evaluated. Changes in the GCC thickness were identified using a manual ROI approach (ROI_M), whereby region(s) of observed or suspected glaucomatous damage were manually identified when using key features from the macular OCT scan on the second visit. Progression was also evaluated using the global GCC thickness and an automatic ROI approach (ROI_A), where contiguous region(s) that fell below the 1% lower normative limit and exceeded 288 μm^2 in size were evaluated. Longitudinal signal-to-noise ratios (SNRs) were calculated for progressive changes detected by each of these methods using individualized estimates of test–retest variability and age-related changes, obtained from 303 glaucoma and 394 healthy eyes, respectively.

Results: On average, the longitudinal SNR for the global thickness, ROI_A and ROI_M methods were $-0.90\ y^{-1}$, $-0.91\ y^{-1}$, and $-1.03\ y^{-1}$, respectively, and was significantly more negative for the ROI_M compared with the global thickness ($P = 0.003$) and ROI_A methods ($P = 0.021$).

Conclusions: Progressive glaucomatous macular GCC changes were optimally detected with a manual ROI approach.

Translational Relevance: These findings suggests that an approach based on a qualitative evaluation of OCT imaging information and consideration of known patterns of damage can improve the detection of progressive glaucomatous macular damage.

Introduction

Glaucoma is an optic neuropathy characterized by the progressive loss of retinal ganglion cells (RGC). The highest density of RGC can be found in the central portion of the retina. For example, the central ±8° from fixation, referred to here as the macular region, represents approximately 2% of the retinal area, but contains over 30% of the RGC.[1] Recent evidence from optical coherence tomography (OCT) suggests that macular damage is more common in glaucoma eyes than previously appreciated, especially in the early stages of the disease.[2–7] This is particularly true for RGC in the inferior macula, because the axons of many of the RGC enter the disc in the highly vulnerable inferior quadrant of the disc.[2,7,8] Given that central visual function is crucial for daily

functioning[9] and vision-related quality of life,[10–12] an important goal in the management of patients with glaucoma is the prevention or delay of the development and progression of macular damage. However, this remains a challenging task and the optimal methods for achieving this remains to be established.

With OCT imaging, previous studies have used global trend–based[13,14] and topographic event–based analyses[15] of the ganglion cell plus inner plexiform layer (GCIPL) thickness in the macular region as a method for detecting progressive changes. However, these methods do not account for the nature of glaucomatous macular damage when evaluating disease progression. For instance, the current topographic event–based analysis of the GCIPL thickness[15] is agnostic to whether the observed changes resemble known patterns of macular damage and simply defines progression on the basis of a predefined criterion. Progression detected in this manner could therefore occur simply as a result of measurement variability.

Instead, we hypothesize that evaluating progression in regions of glaucomatous macular damage can improve its accuracy, based upon our previous findings that progressive circumpapillary retinal nerve fiber layer (RNFL) thickness changes are better captured by evaluating region(s)-of-interest (ROI).[16,17] Such regions of macular damage are likely better identified by a careful qualitative evaluation of all the available OCT scan information and incorporating prior knowledge about patterns of glaucomatous damage. This qualitative approach is comparable to evaluating the appearance of the optic nerve on fundus biomicroscopy or stereophotographs for the presence of glaucomatous damage. In addition, we have previously shown that a qualitative approach is superior, as compared with summary metrics, in the detection of glaucomatous damage.[7]

Thus, the aim of this study was to determine whether a manual ROI approach, involving the aforementioned qualitative evaluation, could capture progressive glaucomatous macular damage more accurately than the common current approach of using a global thickness measure. We also evaluated whether progression could be as effectively captured in regions of automatically identified macular damage, compared with the manual ROI approach. To ensure an equivalent comparison of these approaches, we evaluated progression by calculating longitudinal signal-to-noise ratios (SNRs)[18] after adjusting for normal age-related changes and measurement variability.

Methods

Participants

This study included participants as part of a prospective study to improve the understanding of the role of OCT imaging in glaucoma. It was approved by the institutional review boards of Columbia University and New York Eye and Ear Infirmary of Mount Sinai, and adhered with the Declaration of Helsinki and the Health Insurance Portability and Accountability Act. All participants provided written informed consent after an explanation of the study.

The participants were all considered to have suspected or established glaucoma on the basis of a comprehensive clinical examination by the referring glaucoma specialist (RR). Each eye was required to have a least one reliable visual field test obtained using the Swedish Interactive Threshold Algorithm (SITA) standard 24-2 testing strategy on a Humphrey Field Analyzer II-I (Carl Zeiss Meditec, Inc., Dublin, CA), with a visual field test defined as being unreliable if there were greater than 15% false-positive errors or greater than 33% fixation losses or false-negative errors (except in the latter case when mean deviation [MD] was less than −12 dB). The exclusion criteria for the eyes in this study include any retinal pathology (e.g., epiretinal membrane) that could affect the macular GCIPL or RNFL.

Optical Coherence Tomography Imaging

Volume scans of the macular region, consisting of 512×128 A-scans over a 6×6-mm region centered on the fovea, were obtained for all glaucoma eyes with a spectral-domain OCT device (3D OCT-2000; Topcon, Inc., Tokyo, Japan). Any scan affected by significant eye movement or blink artifacts were considered unreliable, and thus excluded from this study. All eyes were required to have at least two scans that were either, at least 1 year apart to evaluate longitudinal changes (being the "signal" component), or within the same visit to estimate intrinsic measurement variability (or the "noise" component). The eyes that met either of these criteria formed the "longitudinal group" and "variability group," respectively, and an eye was assigned to being in the former if it fulfilled both criteria.

Normative Group for Estimating Age-Related Changes

This study also included one randomly selected eye with a macular volume scan from 394 healthy participants included in a reference database study by the OCT device manufacturer (data were provided by Topcon, Inc.). These eyes formed the "normative group." All eyes were required to be free of any ocular pathology or narrow angles, have a best-corrected visual acuity of 20/40 or better, free of visual field defects consistent with glaucoma also using the SITA Standard 24-2 strategy, and have an intraocular pressure of 21 mm Hg or less. Any participant with a significant medical history that could influence the OCT imaging results was also excluded. The same OCT scan protocol used for these healthy eyes was also used for the glaucoma eyes, although a different spectral-domain OCT device was used (3D OCT-1 Maestro; Topcon, Inc., Tokyo, Japan). The only key difference between the two devices is the scan acquisition speed (27,000 and 50,000 A-scans per second for the 3D OCT-2000 and 3D OCT-1 Maestro, respectively), which is unlikely to have a significant impact on the estimates of age-related change of the RNFL thickness.

Methods for Detecting Progression using the Macular Volume Scan

A customized program written in MATLAB (MathWorks Inc., Natick, MA) was used to manually co-register the two volume scans from the eyes in the longitudinal and variability groups. This was performed using retinal features (such as the blood vessels) on the en face projection images. Once the two scans were co-registered, three methods were used to evaluate progressive changes in the macular ganglion cell complex (GCC) thickness in the eyes within the longitudinal group. The GCC represents the combined thickness of the GCIPL and RNFL, and evaluation of the average GCC thickness within ROI(s) allow both the depth and size of the progressive changes to be captured.

The first method, global thickness, compares the change in the global GCC thickness within a region with a radius of 8° centered on the fovea, excluding a central region with a radius of 2°. This annulus is referred to as the "macular region" in this study. The second method, an automatic ROI approach (ROI_A), compares the change in contiguous regions of GCC thickness that fall below the 1% lower normative limits and exceed 288 μm^2. Note that the minimum size of this area is equivalent to the minimum size of a region used for defining progression with local event-based analysis of both the optic disc RNFL and macular GCIPL in previous studies.[15,19] The third method, a manual ROI approach (ROI_M), compares the change in a manually outlined region of observed or suspected glaucomatous damage. Such regions were identified after reviewing the information available from the volume scan (as illustrated in Fig. 1), including the following: (1) an en face projection image; (2) an en face slab image of the inner retina, showing the average intensity of a 52-μm slab below the inner limiting membrane[20]; (3) a macular RNFL thickness plot; (4) an RGC+ thickness plot; (5) a GCC thickness plot; (6) a corresponding thickness deviation probability plot; and (7) three horizontal and three vertical B-scans taken through the fovea and 3 mm on either sides. One experienced grader reviewed the information from the volume scans and manually outlined ROIs for all the eyes using another custom written program on MATLAB. Note, it is possible for an eye not to have a region that satisfied the criterion for the ROI_A method, and/or to have a region of observed or suspected glaucomatous damage for the ROI_M method. In such cases, the entire macular region was considered the ROI for evaluating progression, and therefore the global GCC thickness was used.

An example showing the difference between the ROI identified by the ROI_A and ROI_M is presented in Figure 2. For this eye, a larger ROI_M was selected manually based on the suspicion of glaucomatous macular damage beyond what is outlined by the contiguous ROI_A of GCC thickness that falls below the 1% normative limits.

Longitudinal Signal-to-Noise Ratio Calculation

To ensure an equivalent comparison between the three methods, it was important to account for between-method and between-individual differences in measurement variability, as well as normal age-related changes of the GCC thickness. This was achieved through using longitudinal SNRs[18] as the primary outcome measure. Note, therefore that longitudinal SNRs are simply normalized values of the rate of change relative to measurement variability, used for comparing the different methods evaluated. Note also, that they do not provide a measure of extent of change, as SNRs or *Z*-scores typically do.

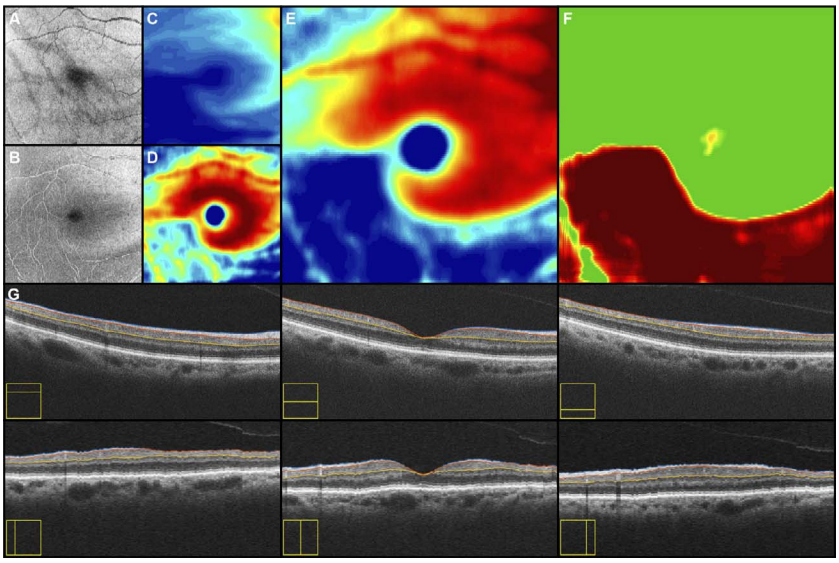

Figure 1. Information from the macular volume scan that was used for the manual identification of a ROI_M, including: (A) an en face projection image, (B) an en face slab image (created from a slab 52-μm below the inner limiting membrane), (C) an RNFL thickness plot, (D) a GCIPL thickness plot, (E) a GCC (being the combination of the RNFL and GCIPL) thickness plot, (F) a GCC thickness deviation probability plot, and (G) three horizontal scans 3 mm above, at, and 3 mm below the fovea and three vertical scans 3 mm temporal, at, and 3 mm nasal to the fovea (with the *yellow boxes* on the *bottom left corner* of each scan indicating the scan position).

Therefore, they should not be used to determine the progression status of an individual eye.

Longitudinal SNRs were calculated for each method (m) by first obtaining an estimate of the rate of change by dividing the difference in GCC thickness between the two visits (δ) by the follow-up interval (t). An estimate of age-related change (a) was then subtracted from this estimate, and the resulting value was divided by an estimate of variability (σ), to obtain the longitudinal SNR_m In particular,

$$SNR_m = \frac{(\delta_m/t) - a_m}{\sigma_m} \quad (1)$$

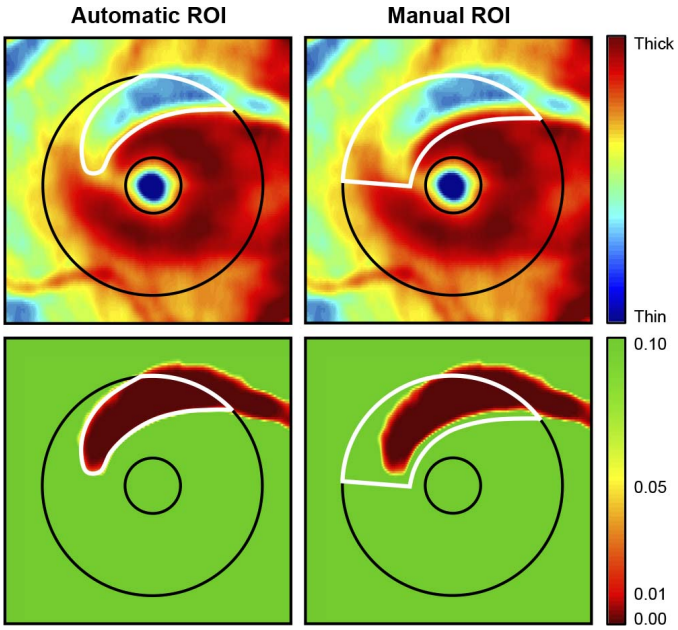

Figure 2. An example illustrating the difference between the ROI (shown using *white outlines*) identified automatically (*left column*) and manually (*right column*), shown on GCC thickness plots (*top row*) and thickness deviation probability plots (*bottom row*); note that their corresponding *scale bars* are shown on the *right*.

Given that this ROI approach evaluates change in regions that are unique to each eye, estimates of age-related change and measurement variability for these specific regions are required. This process is illustrated in Figure 3, using an example of an eye with a ROI in the superior macular region, which is shown as a green outline in the left panel. To obtain individualized estimates of the normal rates of age-related macular GCC change, the average GCC thickness of the same ROI, within the green boundary in the case of Figure 3, for each of the eyes in this normative group were obtained. The slope of a linear regression model fitted to these values against age provided the particular ROI-specific cross-sectional estimate of age-related change (middle panel of Fig. 3). Region-specific estimates of variability were then obtained by calculating the standard deviation (SD) of the test–retest differences of the average GCC thickness of the ROI for all eyes in the variability group (right

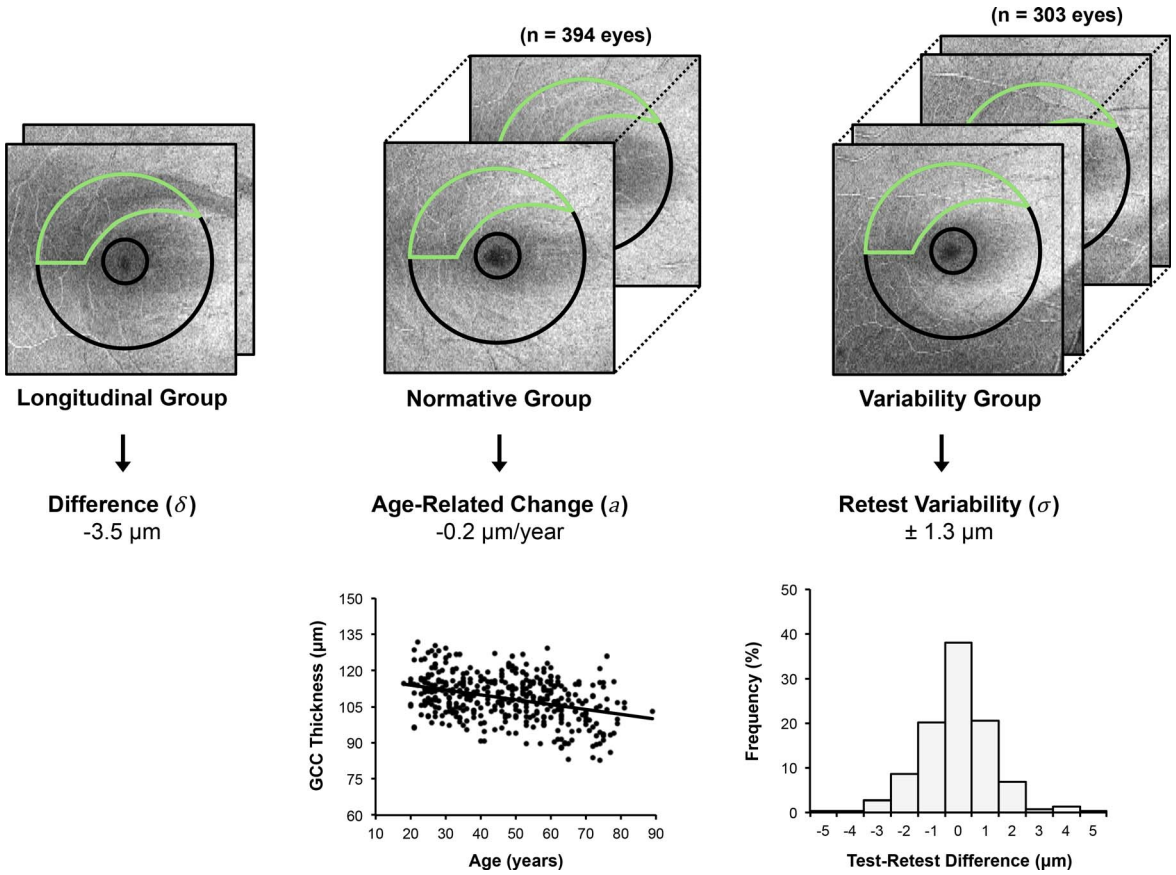

Figure 3. Illustration of the method used to obtain an estimate of age-related change and measurement variability of a ROI (*green outline*) for the GCC thickness in a central region with a radius of 8° (*black circle*) for an eye in the longitudinal group (*left section*). The estimate of age-related change was derived by calculating the slope of a linear regression fit between the average GCC thickness of the ROI and age for all eyes in the normative group (*middle section*). The region-specific variability estimate was then derived using the SD of the test–retest differences of the average GCC thickness for all the eyes in the variability group (*right section*).

panel of Fig. 3; and see Statistical Analysis section). This process was then repeated for each eye in the longitudinal group.

Statistical Analysis

A random intercept model, which is a type of linear mixed model, was used to determine the SD of the test–retest differences for a given ROI, because the variability cohort included some participants where both their eyes were included. The same model was also used to compare the difference in the average longitudinal SNR between the methods, specifying nesting of the methods within eyes and within participants. The statistical analyses were performed using both MATLAB and Stata (StataCorp LP, College Station, TX).

Results

Participant Characteristics

A total of 146 eyes from 96 participants with established or suspected glaucoma were included in the longitudinal group. The mean ± SD of their age and follow-up duration were 57 ± 14 years (range, 19–82 years) and 1.7 ± 0.6 years (range, 1–3 years), respectively. The median (interquartile range) visual field MD and pattern standard deviation (PSD) of these eyes were −2.02 dB (−4.37 to −0.48 dB) and 1.88 dB (1.54 to 4.97 dB), respectively. A total of 303 eyes from 193 participants with suspected or established glaucoma were also included as part of the variability group. They were on average 59 ± 14-years old (range, 23- to 89-years old), and the median (interquartile range) visual field MD and PSD of

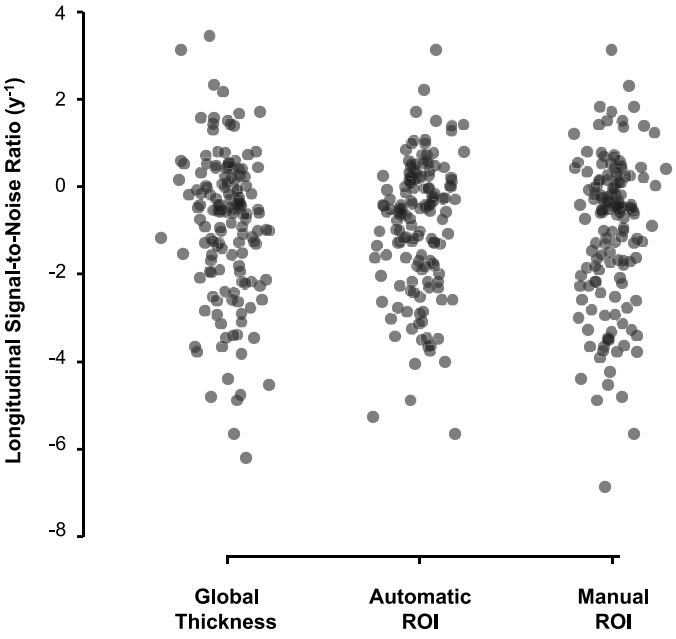

Figure 4. Distributions of the longitudinal SNR of the global thickness, automatic and manual ROI approaches toward capturing changes in the macular GCC thickness over time. Note that more negative values indicate a greater extent of thinning over time relative to normal age-related changes and measurement variability.

these eyes were −2.48 dB (−5.91 to −0.87 dB) and 2.23 dB (1.55 to 6.29 dB), respectively.

Comparison of the Longitudinal Signal-to-Noise Ratio Between Methods

Among the 146 eyes with established or suspected glaucoma evaluated, 74 eyes (51%) satisfied the criterion for the ROI_A method and 79 eyes (54%) where at least one ROI was manually outlined using the ROI_M method, showing how glaucomatous macular damage was either suspected or observed in a notable percentage of eyes in this cohort. The distributions of the longitudinal SNRs for the three methods are shown in Figure 4. On average, the longitudinal SNRs for the global thickness method, ROI_A and ROI_M were −0.90 y^{-1}, −0.91 y^{-1}, and −1.03 y^{-1}, respectively. Note, more negative longitudinal SNRs indicate a greater extent of GCC thickness loss detected relative to age-related change and measurement variability. The longitudinal SNR for the ROI_M was significantly more negative than the ROI_A (−0.12 y^{-1}; 95% confidence interval [CI] = −0.23 to −0.02 y^{-1}; $P = 0.021$) and global GCC thickness (−0.13 y^{-1}; 95% CI = −0.21 to −0.05 y^{-1}; $P = 0.003$), consistent with our hypothesis that the ROI_M was the optimal method for detecting macular GCC loss. Furthermore, the longitudinal SNR for the ROI_A was not significantly more negative than global GCC thickness (−0.01 y^{-1}; 95% CI = −0.11 to 0.10 y^{-1}; $P = 0.903$).

Examples of Findings in this Study

The four examples in Figures 5 and 6 illustrate the findings. The first two (Fig. 5) demonstrate two cases where the ROI_M method detected a more negative longitudinal SNR than the ROI_A and global thickness methods. The first case (Fig. 5A) shows an eye where the superior macular ROI_M was manually outlined (white border) based upon the vertical asymmetry of the GCC thickness map on the second visit. The region of abnormality (below the 1% lower normative limit) on the GCC thickness deviation plot was not greater than 288 μm^2, to meet the inclusion criteria of the ROI_A method. However, changes in the GCC thickness occurred in the ROI_M over time, with its changes reflected by the longitudinal SNRs of the ROI_M (−3.9 y^{-1}) and global thickness and ROI_A (−3.2 y^{-1}) methods. This case provides an example of an eye where the ROI_A fails to detect early glaucomatous macular damage, and that the ROI_M provides a more targeted evaluation of local progressive change than a global metric. The second case (Fig. 5B) shows an eye with an inferior arcuate defect involving the macular region. The region manually outlined in white by the ROI_M method was larger than the ROI_A of abnormality below the 1% (red) lower normative limit on the GCC thickness deviation plot (lower middle panel). Changes in the global GCC thickness also occurred primarily in this entire region over time, and thus the longitudinal SNR of the ROI_M (−3.6 y^{-1}) was more negative than the ROI_A method (−2.7 y^{-1}), and both were more negative than the global thickness method (−1.4 y^{-1}). This case provides an example where the ROI_A underestimates the extent of glaucomatous macular damage captured by the ROI_M method, and how the global thickness method underestimates local progressive changes captured by both ROI methods.

The next two examples illustrate cases in which either the ROI_A (Fig. 6A) or global thickness (Fig. 6B) method worked better than the other, but the ROI_M method was still the optimal method. The third case (Fig. 6A) shows an eye with an inferior arcuate defect that affects most of the inferior macular region. The region manually outlined closely corresponded to the region automatically identified as falling below the 1% lower normative limits. GCC changes over

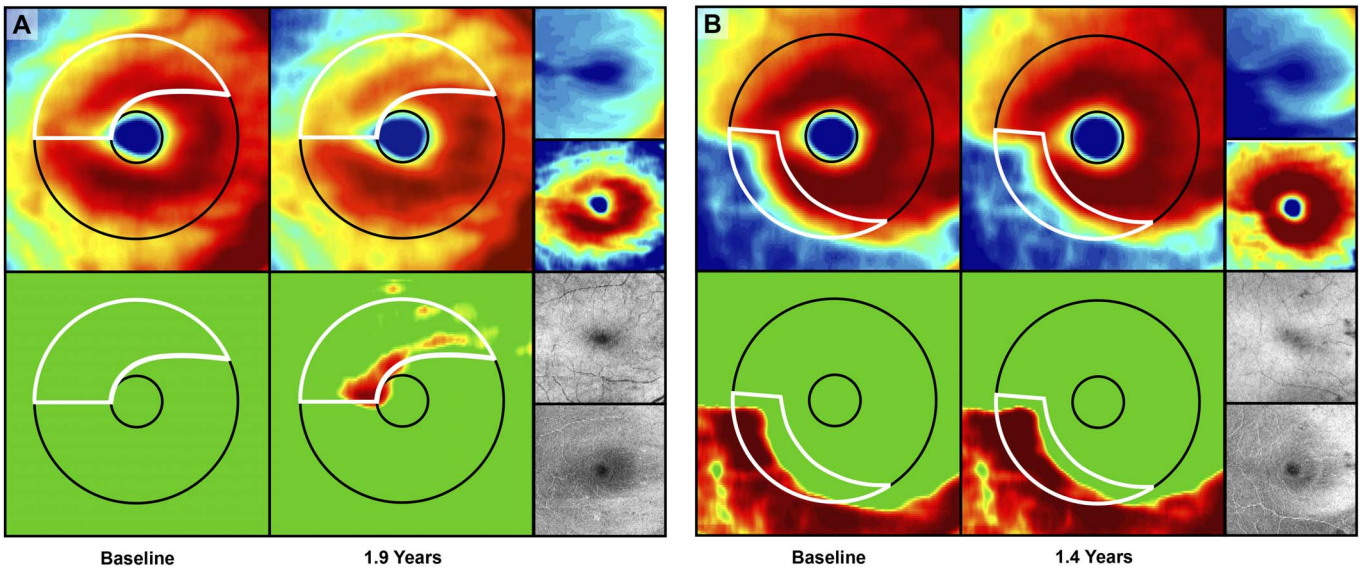

Figure 5. Two examples illustrating how the ROI_M method (shown as *white outlines*) better captured progressive GCC thickness loss in the macular region (outlined by the *large black circles*, excluding the region outlined by the *smaller black circles*) than the ROI_A or global thickness methods. In each example, the *left* and *middle columns* show the GCC thickness (*top*) and GCC thickness deviation plots (*bottom*) for the first and second visits, respectively. The *right column* shows a RNFL thickness plot, macular GCIPL thickness plot, en face projection image and en face slab image (from a slab 52 μm below the inner limiting membrane) from *top* to *bottom*, respectively.

time that occurred in this area were thus similar for the ROI_M ($-4.0\ y^{-1}$) and ROI_A methods ($-3.8\ y^{-1}$), and were more negative than the global thickness method ($-3.0\ y^{-1}$). The fourth case (Fig. 6B) shows an eye with reduced GCC thickness primarily in the inferior macular region, but which also affected the superior macular region to a lesser extent. The latter was suspected on the basis of the vertical asymmetry

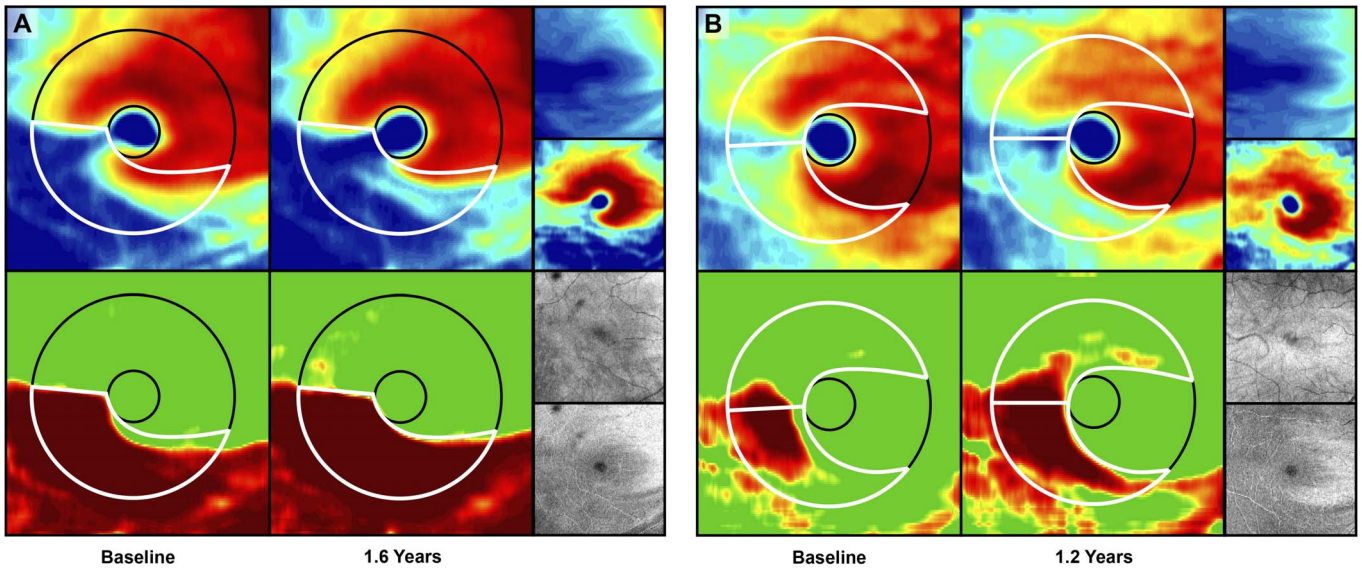

Figure 6. Examples illustrating cases where the ROI_A detected progressive change of the GCC thickness over time in the macular region more effectively than the global thickness approach (outlined by the *large black circles*, excluding the region outlined by the *smaller black circles*; [A]) and vice versa (B), although the ROI_M (shown as *white outlines*) were still optimal in these cases. In both examples, the *left* and *middle columns* present the GCC thickness (*top*) and GCC thickness deviation plots (*bottom*) from the first and second visits, respectively. The *right column* presents the RNFL thickness plot, macular GCIPL thickness plot, en face projection image and en face slab image (from a slab 52 μm below the inner limiting membrane) from *top* to *bottom*, respectively.

in the GCC thickness appearing to be present—especially in the nasal portion of the macular region—and the presence of GCC thickness deviation abnormalities in the superior-temporal region beyond the horizontal midline. Both the superior and inferior macular regions indeed exhibited GCC loss over time and both the ROI_M ($-7.0\ y^{-1}$) and global thickness methods ($-6.4\ y^{-1}$) were more negative than the ROI_A method ($-5.4\ y^{-1}$). The better performance of the global thickness method is likely attributed to the observation that a large proportion of the macular exhibited change over time, while the ROI_A method underestimated the extent of the glaucomatous macular damage.

Discussion

We hypothesized that evaluating progression in regions of glaucomatous damage within the macula could improve its accuracy, and our findings indeed revealed that a manual ROI approach performed better than the commonly used measure of global thickness. Furthermore, our findings also showed that the evaluation with manually determined ROIs—which considers known patterns of glaucomatous macular damage—also performed better than automatically identified ROIs that rely on a predefined criterion. These findings suggest that progressive glaucomatous macular damage can be better detected by using the full wealth of information available on OCT imaging.

The detection of progressive macular damage in glaucoma is paramount, given that such damage can result in central visual dysfunction that affects daily functioning[9] and vision-related quality of life.[10–12] As such, new methods for detecting its progressive changes on OCT imaging have been evaluated in recent years.[13–15] However, these methods do not attempt to distinguish between glaucomatous and nonpathological patterns of loss. For instance, progression is considered to have occurred simply if a statistically significant negative slope is present for macular GCIPL thickness values over time when using global trend–based analyses.[13,14] It is also considered to have occurred if a statistically significant change from baseline values in a contiguous region exceeding a minimum size (regardless of its location or pattern) is present with topographic event–based analyses.[15] Instead, our findings demonstrate that the detection of progression could be further improved by evaluating changes in regions of observed or suspected glaucomatous macular damage using the manual ROI approach, which was rapid to perform. Note, however, that this does not mean that topographic trend– or event-based analyses are not useful, but rather that such analyses are likely more effective when performed within regions of observed or suspected glaucomatous damage.

The superiority of the manual ROI approach is likely attributed to the fact that glaucomatous macular damage was more accurately identified based on a careful qualitative evaluation of all the available OCT imaging information while considering its known arcuate patterns of damage. This approach is distinctly different from simply considering damage to be present in regions with a significantly lower GCC thickness relative to normative limits. This is likely because some regions of true glaucomatous damage, especially early damage, can fall within the normative limits and/or fail to meet the predefined criterion of a minimum size of a contiguous region due to the large normal interindividual topographic variation in macular neuroretinal thickness.[21,22] As such, the full topographic extent of the region of macular damage may not be entirely captured by the automatic ROI approach. The two examples shown in Figure 4 provide illustrations of these scenarios. Our finding that the global GCC thickness and automatic ROI_A methods performed similarly also contributes to the notion that the full extent of glaucomatous damage can sometimes be suboptimally captured by a predefined criterion (and thus detected using the global parameter instead, such as in the example shown in Fig. 5B).

These findings suggest that the detection of progressive glaucomatous macular damage is optimal when making full use of the OCT imaging information available and by considering known arcuate patterns of damage. This is likened to a Bayesian approach typically used in the clinical diagnosis of glaucoma, where a constellation of evidence is evaluated against known characteristics of this condition.[23] Furthermore, the advantages of the qualitative evaluation is similar to those gained through a clinical examination of the optic nerve appearance, where a greater extent of information can be derived than simply considering a cup-to-disc ratio measurement.

However, note that the advantages of the manual ROI approach was only inferred from the population-based analyses of the longitudinal SNRs in this study, and thus its clinical implications at the individual level needs to be established in future studies. These analyses using a continuous outcome measure allow potential true differences between the performance of

different methods to be detected with a substantially greater statistical power compared with an individual-based, binary outcome of progression status.[24] This is especially the case when evaluating methods for detecting glaucoma progression, because many patients under routine clinical care often progress slowly.[25] As a result, large cohorts of participants seen over long follow-up durations would be needed to detect such potential true differences if individual-based, dichotomous outcomes were used. Instead, the population-based analyses performed in this study provide a powerful framework for a proof-in-principle evaluation of this manual ROI approach, encouraging future investigations.

Several other limitations should also be noted when interpreting the findings of this study. First, eyes in the longitudinal cohort had a relatively short duration of follow-up (average of 1.7 ± 0.6 years) and were evaluated over only two visits. However, increasing the number of visits and/or duration of follow-up would only improve the precision of the longitudinal SNR estimates and would unlikely change the conclusions made in this study. Furthermore, the relatively large number of eyes evaluated longitudinally compensates for the limited follow-up duration and visits. Second, short-term within-session estimates of variability were used rather than short-term between-session estimates, which would provide a more ideal estimate of the variability expected for the eyes evaluated in the longitudinal cohort. However, this is also unlikely to affect the conclusions reached in this study, because the variability estimates used when calculating the longitudinal SNRs were obtained from the same eyes with each method. Finally, it remains to be determined whether other definitions of automatically identified ROIs could improve the automatic ROI approach.

In conclusion, this study demonstrated that progressive glaucomatous macular GCC thinning was optimally detected by evaluating regions of observed or suspected damage identified when performing a qualitative evaluation of the OCT imaging results. This was superior to use of a global metric and automatically identified ROIs, in agreement with our previous observations that a qualitative approach is also superior when compared with summary metrics in the detection of glaucomatous damage.[7]

Acknowledgments

Supported by a National Institutes of Health Grant R01-EY-02115 (DCH), Lary Stromfeld Research Fund of NYEEI (RR), and a National Health & Medical Research Council Early Career Fellowship (#1104985; ZW).

Disclosure: **Z. Wu**, None; **D. Weng**, None; **A. Thenappan**, None; **R. Ritch**, None; **D.C. Hood**, Topcon, Inc (F, C), Heidelberg Engineering (F)

References

1. Curcio CA, Allen KA. Topography of ganglion cells in human retina. *J Comp Neurol*. 1990;300:5–25.
2. Hood DC, Raza AS, de Moraes CGV, et al. Glaucomatous damage of the macula. *Prog Retin Eye Res*. 2013;32:1–21.
3. Hood DC, Slobodnick A, Raza AS, et al. Early glaucoma involves both deep local, and shallow widespread, retinal nerve fiber damage of the macular region. *Invest Ophthalmol Vis Sci*. 2014;55:632–649.
4. Wang DL, Raza AS, de Moraes CG, et al. Central glaucomatous damage of the macula can be overlooked by conventional oct retinal nerve fiber layer thickness analyses. *Trans Vis Sci Tech*. 2015;4(6):4.
5. Grillo LM, Wang DL, Ramachandran R, et al. The 24-2 visual field test misses central macular damage confirmed by the 10-2 visual field test and optical coherence tomography. *Trans Vis Sci Tech*. 2016;5(2):15.
6. Kim YK, Ha A, Na KI, et al. Temporal relation between macular ganglion cell–inner plexiform layer loss and peripapillary retinal nerve fiber layer loss in glaucoma. *Ophthalmology*. 2017;124:1056–1064.
7. Hood DC. Improving our understanding, and detection, of glaucomatous damage: an approach based upon optical coherence tomography (OCT). *Prog Retin Eye Res*. 2017;57:46–75.
8. Hood DC, Raza AS, De Moraes CGV, et al. Initial arcuate defects within the central 10 degrees in glaucoma. *Invest Ophthalmol Vis Sci*. 2011;52:940–946.
9. Ramulu P. Glaucoma and disability: which tasks are affected, and at what stage of disease? *Curr Opin Ophthalmol*. 2009;20:92.
10. Abe RY, Diniz-Filho A, Costa VP, et al. The impact of location of progressive visual field loss on longitudinal changes in quality of life of

patients with glaucoma. *Ophthalmology*. 2016; 123:552–557.
11. Blumberg DM, De Moraes CG, Prager AJ, et al. Association between undetected 10-2 visual field damage and vision-related quality of life in patients with glaucoma. *JAMA Ophthalmol*. 2017;125:742–747.
12. Prager AJ, Hood DC, Liebmann JM, et al. Association of glaucoma-related, optical coherence tomography–measured macular damage with vision-related quality of life. *JAMA Ophthalmol*. 2017;135:783–788.
13. Lee WJ, Kim YK, Park KH, Jeoung JW. Trend-based analysis of ganglion cell–inner plexiform layer thickness changes on optical coherence tomography in glaucoma progression. *Ophthalmology*. 2017;124:1383–1991.
14. Leung CK-S, Ye C, Weinreb RN, et al. Impact of age-related change of retinal nerve fiber layer and macular thicknesses on evaluation of glaucoma progression. *Ophthalmology*. 2013;120:2485–2492.
15. Shin JW, Sung KR, Lee GC, et al. Ganglion cell–inner plexiform layer change detected by optical coherence tomography indicates progression in advanced glaucoma. *Ophthalmology*. 2017;124: 1466–1474.
16. Hood DC, Xin D, Wang D, et al. A region-of-interest approach for detecting progression of glaucomatous damage with optical coherence tomography. *JAMA Ophthalmol*. 2015;133: 1438–1444.
17. Thenappan A, De Moraes CG, Wang DL, et al. Optical coherence tomography and glaucoma progression: a comparison of a region of interest approach to average retinal nerve fiber layer thickness. *J Glaucoma*. 2017;26:473–477.
18. Gardiner SK, Fortune B, Demirel S. Signal-to-noise ratios for structural and functional tests in glaucoma. *Trans Vis Sci Tech*. 2013;2(6).
19. Yu M, Lin C, Weinreb RN, et al. Risk of visual field progression in glaucoma patients with progressive retinal nerve fiber layer thinning: a 5-year prospective study. *Ophthalmology*. 2016; 123:1201–1210.
20. Hood DC, Fortune B, Mavrommatis MA, et al. Details of glaucomatous damage are better seen on oct en face images than on oct retinal nerve fiber layer thickness maps. *Invest Ophthalmol Vis Sci*. 2015;56:6208–6216.
21. Sepulveda JA, Turpin A, McKendrick AM. Individual differences in foveal shape: feasibility of individual maps between structure and function within the macular region. *Invest Ophthalmol Vis Sci*. 2016;57:4772–4778.
22. Turpin A, Chen S, Sepulveda JA, McKendrick AM. Customizing structure–function displacements in the macula for individual differences. *Invest Ophthalmol Vis Sci*. 2015;56:5984–5989.
23. Casson RJ, Chidlow G, Wood JP, et al. Definition of glaucoma: clinical and experimental concepts. *Clin Exp Ophthalmol*. 2012;40:341–349.
24. Royston P, Altman DG, Sauerbrei W. Dichotomizing continuous predictors in multiple regression: a bad idea. *Stat Med*. 2006;25:127–141.
25. Chauhan BC, Malik R, Shuba LM, et al. Rates of glaucomatous visual field change in a large clinical population. *Invest Ophthalmol Vis Sci*. 2014;55:4135–4143.